A modified multiple tension upward infiltration method to estimate the soil hydraulic properties

D. Moret-Fernández[a], B. Latorre[a], C. Peña-Sancho [a], T.A. Ghezzehei [b]

[a] Departamento de Suelo y Agua, Estación Experimental de Aula Dei, Consejo Superior de Investigaciones Científicas (CSIC), PO Box 13034, 50080 Zaragoza, Spain

[b] Life and Environmental Sciences, University of California Merced, 5200 N. Lake Rd., Merced CA 95343, United States.

* Corresponding author. E-mail: david@eead.csic.es Tel.: (+34) 976 71 61 40

Abstract

Determination of saturated hydraulic conductivity, K_s, and the shape parameters α and n of the water retention curve, $\theta(h)$, is of paramount importance to characterize the water flow in the vadose zone. This work presents a modified upward infiltration method to estimate K_s, α and n from numerical inverse analysis of the measured cumulative upward infiltration (CUI) at multiple constant tension lower boundary conditions. Using the HYDRUS-2D software, a theoretical analysis on a synthetic loam soil under different soil tensions (0, 0-10, 0-50, and 0-100 cm), with and without an overpressure step of 10 cm high form the top boundary condition at the end of the upward infiltration process, was performed to check the uniqueness and the accuracy of the solutions. Using a tension sorptivimeter device, the method was validated in a laboratory experiment on five different soils: a coarse and a fine sand, and a 1-mm sieved loam, clay loam and silt-gypseous soils. The estimated α and n parameters were compared to the corresponding values measured with the TDR-pressure cell method. The theoretical analysis demonstrates that K_s and $\theta(h)$ can be simultaneously estimated from measured upward cumulative infiltration when high (> 50 cm) soil tensions are initially applied at the lower boundary. Alternatively, satisfactory results can be also obtained when medium tensions (< 50 cm) and the K_s calculated from the overpressure step at the end of the experiment are considered. A consistent relationship was found between the α ($R^2 = 0.86$, $p < 0.02$) and n ($R^2 = 0.97$, $p < 0.001$) values measured with the TDR-pressure cell and the corresponding values estimated with the tension soptivimeter. The error between the α (in logarithm scale) and n values estimated with the inverse analysis and the corresponding values measured with pressure chamber were 3.1 and 6.1%, respectively.

Keywords: Disc infiltrometer; Hydraulic conductivity; Water Retention Curve; HYDRUS

1. Introduction

The hydraulic conductivity, K, and the water retention curve, $\theta(h)$ are the main soil properties that determine the water flow in the vadose zone. Many laboratory methods for determining these properties are cited in the literature. For instance, the saturated K can be measured by using either the constant head or the falling-head method (Klute and Dirksen, 1986). The reference laboratory method employed to determine $\theta(h)$ is the pressure extractor (Klute, 1986). A pressure plate extractor referred to as a "Temple cell" is commonly used for suctions up to -100 kPa. For higher matric suctions (typically -1500 kPa) more robust pressure cells are used (Wand and Benson, 2004).

Numerical methods involving the inverse solution of the Richards equation are increasingly used as alternative procedures to estimate the soil hydraulic properties (Simunek et al., 1996, Simunek and van Genuchten, 1997). An advantage of this approach is that the retention and hydraulic conductivity functions are estimated simultaneously from transient flow data (Rashid et al., 2015). For instance, Hudson et al. (1996) suggested estimating the soil hydraulic properties from the inverse analysis of an upward flow experiment for laboratory conditions. In this case, a constant flux of water at the bottom of the soil sample was imposed, and the pressure head inside the sample was measured with tensiometers. Because the flux was independent of the soil properties, this method allowed excluding the flux as a parameter to be optimized. This method was subsequently modified by Simunek et al. (2001), who estimated the soil hydraulic parameters from the inverse analysis of a constant head at the lower boundary of a 10-cm-long soil core, followed by an evaporation experiment. This laboratory technique was next improved by Young et al. (2002) who, using a Mariotte system and tensiometers installed along a 15-cm-long soil column, allowed simultaneous measurements of water upward flow at negative pressure head (-0.3 and -0.8 kPa) and changes in soil pressure head. Using the pressure head and the cumulative flux data as auxiliary variables of the objective function, the soil hydraulic parameters were calculated with HYDRUS-1D from the best optimization of the objective

function. The inverse analysis of a multiple head tension water flow has been also successfully applied on the infiltrometer technique (Simunek and van Genuchten, 1997). Using numerical simulations, these authors demonstrated that the method could provide information on the hydraulic conductivity and the water retention curve. Although this multiple tension disc infiltrometer technique has been successfully employed in experimental studies (Ramos et al., 2006; Rashid, et al., 2015), the long time needed to conclude a measurement may limit its use if, for instance, a large scale or intensive characterization of soils is needed. In these cases, sampling of undisturbed soil cores to be analysed in laboratory can be preferable.

As above referred, methods to estimate the soil hydraulic properties from the inverse analysis of an upward infiltration processes are scarce. The capillary rise processes are described by bundle models, however, these models can not be correct at all because a real soil can support flow in any direction. (Hunt et al., 2013). Taking into account these limitations, the objective of this study was to determine if the soil hydraulic properties can be derived from the inverse analysis of measured cumulative upward infiltration at multiple imposed tensions at the lower boundary. To this end, different scenarios of upward infiltration at different tensions at the bottom of a soil core were studied. In a first step, a theoretical analysis to verify the most favourable range of soil tensions to be applied was performed using HYDRUS-simulated data. It also determined if additional easily obtainable information, such as the water flow at positive pressure head, allowed improving the identifiability of the unknown parameters. In a second phase, a new laboratory device, the tension soprtivimeter, was presented to test this technique. To this end, the hydraulic properties estimated with this method on two different sands and three sieved soils with different textural characteristics were compared to the corresponding soil properties measured with an independent method.

2. Material and methods

2.1 Theory

2.1.1 Water flow in one-dimension

The governing flow equation for one-dimensional Darcian flow in a variably saturated rigid porous medium is given by the following form of the Richards equation

$$\frac{\partial \theta}{\partial t} = \frac{\partial}{\partial z}\left(K \frac{\partial h}{\partial z} + K \right) \quad (1)$$

where θ is the volumetric soil water content [L^3 L^{-3}], h is the soil-water pressure head [L], K is the hydraulic conductivity [L T^{-1}], z is a vertical coordinate (L) positive upward, and t is time [T]. In our case, a constant water content profile corresponding to an air dry soil is used as initial condition. The boundary condition corresponds to a variable soil tension at the bottom of the soil sample and atmospheric conditions at the top. The evaporation rate is null and once the column is saturated a maximum tension of 0 cm is considered constant on the top soil layer. The soil hydraulic functions used are described by the van Genuchten – Mualem conductivity relationship (van Genuchten, 1980)

$$S_e(h) = \frac{\theta(h) - \theta_r}{\theta_s - \theta_r} = \left[1 + (\alpha h)^n\right]^{-m} \quad (2)$$

$$K(S_e) = K_s S_e^l \left[1 - \left(1 - S_e^{1/m}\right)^m\right]^2 \quad (3)$$

where S_e, is the effective saturation [−], θ_s and θ_r are the saturated and residual water contents, respectively [L^3 L^{-3}], K_s is the saturated hydraulic conductivity [L T^{-1}], n [−] and α [L^{-1}] are shape parameters, and m=1−1/n. Similarly to previous works (Simunek et al., 1996; Simunek and van Genuchten et al. 1997; Simunek et al. 1998; Young et al. , 2002), the pore-connectivity parameter, l , was fixed to 0.5. Because θ_r and θ_s can be easily measured at the beginning and end of the experiment, respectively, the hydraulic characteristics defined by Eq. (2) and (3) were reduce to three

unknown parameters: α, n and K_s. In this case, Eq. (2) and (3) represent wetting branches of the unsaturated hydraulic properties.

For saturated soils and steady state condition, Eq (1) is reduced to Darcy's law (Lichtner et al., 1996)

$$q = -K_s \frac{dH}{dz} \tag{4}$$

where q is the water flux density[L T^{-1}] and H=h+z is the total head. Note that for saturated soils h>0.

2.1.2. Inverse analysis

The hydraulic parameters (α, n and K_s) were estimated by minimizing an objective function, $\Phi(K_s, \alpha, n)$, that represents the difference between the simulated and the experimental (or theoretical) data, such as the cumulative upward infiltration:

$$\Phi(K_s, \alpha, n) = \sqrt{\frac{\sum_{i=1}^{n_i} w_i [c_e(t_i) - c_s(t_i)]^2}{n-1}} \tag{5}$$

where n_i is the number of measured (c,t) values, $c_e(t_i)$ and $c_s(t_i)$ are specific measurements at time t_i and the corresponding model prediction for the vector of optimized parameters, respectively, and w_i is the weight associated a particular measurement set or point. In this study, we assumed that the weighting coefficient w_i was equal to one. Minimization of the objective function Φ was accomplished by a brute-force search (Horst and Romeijn, 2002), that enumerates all possible candidates of the hydraulic parameters to a certain precision and selecting the best result. This reference method, that requires considerable computing power, was used to study the properties of the solution space.

2.2. Numerical Experiments

The multiple tension upward infiltration data used in this work were generated numerically with the HYDRUS-2D software (Simunek et al., 1996). Although these simulation can be satisfactorily performed with HYDRUS-1D, the 2D version was chosen because it is more general A loam soil textural group as estimated by Carsel and Parrish (1988) was used during the simulations. The soil hydraulic parameters of the hypothetical loam were: θ_r = 0.078 $m^3\ m^{-3}$, θ_s = 0.43 $m^3\ m^{-3}$, α = 0.036 cm^{-1}, n = 1.56 and K_s = 0.017333 cm s^{-1} (Simunek et al., 2008). The soil volume was discretized as a cylinder (radius of 2.5 cm and high of 5 cm), covering the axisymmetric plane with a 2-D triangular mesh of 1034 cells. Previous numerical analysis demonstrated that, under this discretization, the solution was grid independent. The initial water content of the homogeneous and isotropic soil was 0.08 $m^3\ m^{-3}$. Atmospheric condition was imposed at the top boundary and a null evaporation rate was considered. Four different scenarios of pressure heads at the bottom boundary condition were imposed (Table 1): 0, -10 and 0, -50 and 0, and -100 and 0 cm of pressure heads. The same scenarios were again repeated but including an overpressure of 10 cm at the cylinder base during the last 30 min. Once the column was saturated, a maximum tension of 0 cm was simulated constant on the top soil layer. Taking into account all above considerations, a total of 8 different scenarios were considered. Figure 1 shows an example of multiple tension cumulative upward infiltration generated by HYDRUS-2D for the different scenarios of Table 1.

Forward simulation was performed using HYDRUS-2D to predict the outcomes of the synthetic experiments. The three unknown hydraulic parameters α, n and K_s were varied over wide ranges (0.01 to 0.1 cm min^{-1}, 0.01 to 0.1 cm^{-1}, and 1.1 to 2.9, for α, K_s and n, respectively) encompassing the true (but assumed unknown) values. K_s and α were logarithmically spaced.

The degree of mismatch between the predictions and the synthetic experimental data were computed using the objective function $\Phi(K_s, \alpha, n)$ given in Eq. (5). The values of the objective functions were summarized as contours (response surfaces) for the three possible combinations: K_s-n,

α-n, and K_s-α. The parameter combinations for each response surface were calculated on a rectangular grid. Each parameter was discretized into 140 points resulting in 19600 grid points for each response surface.

Under real situations, experimental data is subject to several sources of uncertainty (i.e. water level measurement, initial and final water content, etc.), which are propagated to the hydraulic parameters estimates as well. For these synthetic experiments we considered uncertainty due to water level measurement and its influence on the upward infiltration data. This uncertainty arises due to the accuracy of the water level measurement sensor, and depends on the ratio of the water supply reservoir diameter to soil cylinder diameter. A preliminary experiment performed with a ±0.5 psi pressure transducer installed in a 2.34 cm-diameter water reservoir and connected to a 5 cm-diameter soil cylinder resulted in a soil water infiltration measurement uncertainty less than ±0.1 mm. To translate this experimental error, a sensitivity analysis was performed around each inverse solution as part of a first order uncertainty analysis. The change of the objective function (Eq. 5) associated to the uncertainty source was first calculated and superimposed on the response surfaces in the form of a contour line (0.1 mm).

2.3. Experimental setup

2.3.1. Tension sorptivimeter

To test this alternative method, a device for cumulative upward infiltration measurements, which will be called from now on tension sorptivimeter, was used (Fig. 2). This device, which is a inverted tension disc infiltrometer, consisted on a stain steel cylinder (5 cm- internal diameter -i.d.- and 5 cm-high) placed on a coarse porous base (5 cm i.d.), which was contained in an aluminum receptacle of 10 cm diameter. The top of the porous base was covered with a 10 μm pore size nylon mesh. Experimental testing revealed that this pore size mesh can supply a maximum soil tension of about 30-45 cm. The base of the cylinder was hermetically closed against the nylon mesh and the aluminum

receptacle, and it was connected to a water-supply reservoir (30 cm high and 2.33 cm i.d.). The water reservoir was connected to a bubbling tower that had a mobile tube that imposed a negative pressure head (h) at the base of the cylinder (Fig. 2). A ±0.5 psi differential pressure transducer (PT) (Microswitch, Honeywell), connected to a datalogger (CR1000, Campbell Scientist Inc.), was installed at the bottom of the water-supply reservoir (Casey and Derby, 2002).

To setup the tension sorptivimeter, the porous base plus nylon mesh should be firstly saturated. To this end, the tube of the bubble tower was removed and the air-inlet tube of the water reservoir was levelled up to the top of the porous base. Once the porous base was saturated, all air trapped between the nylon mesh and the porous base was removed with a syringe. Next, the mobile tube of the bubbling tower was placed at the desired depth, and a negative pressure head was generated in the water reservoir with a syringe (Fig. 1). The desired tension was reached when the bubbling tower started to bubble up. Then, a volume of 100 cm^3 of soil was carefully dumped into the cylinder. At this point, the bubbling tower started to bubbling up, which indicated the soil started to take water. The successive tensions were reached by moving up the mobile tube of the bubbling tower. The last soil tension corresponded to the soil saturation point, in which the mobile tube of the bubbling tower was completely removed. Once the tension in the porous base was zero, the overpressure step was reached by raising the water reservoir to a desired height. The soil column was considered saturated when a water sheet was observed on the top of the cylinder. The excess of water that flowed thought the soil column due to overpressure step was drained by gravity by the edges of the cylinder. The total pressure drop, ΔH, (Eq. 4) was calculated as the distance between the air-inlet tube of the reservoir and the top soil cylinder surface. The saturated hydraulic conductivity (K_s) was calculated from the overpressure section of the simulated cumulative upwards infiltration according to Eq.(4). During the experiment, the water losses due to evaporation were considered negligible. The initial water content was gravimetrically measured and the final water content corresponded to the saturated soil conditions.

2.3.2. Laboratory testing

The method was tested in laboratory on five soils with different textural characteristics (Table 2): a coarse (250-500 μm of grain size) and a fine (80-160 μm of grain size) sand, and a 1-mm sieved loam, clay loam and silt-gypseous soil. The experiment consisted on an upward infiltration process followed by an overpressure step once the wetting front arrived to the top of the soil core. The pressure heads applied from the bottom of the core and the corresponding infiltration times are shown in Table 2. The K_s was measure by applying the Darcy's law to the overpressure step, and the $\Phi(K,\alpha,n)$ response surfaces were calculated, when needed. To this end, a rectangular grid discretized into 70 discrete points, which results in 4900 grid points, were used. The value used in the inverse analysis ranged from to 0.01 to 1 cm s^{-1} and cm^{-1} for K and α, respectively, and from 1.1 to 3.5 for n. The van Genuchten (1980) α and n parameters estimated by inverse optimization of the soil water upward infiltration curves were compared with the corresponding parameters estimated from the water retention curves measured with the TDR-pressure cell method (Moret-Fernández et. al, 2012). The wetting branch of the water retention curve was estimated in the sands. In these cases, pressure heads of 0.3, 0.5, 0.1, 0.2, 0.3, 0.4, 0.5 and 0.65 kPa were applied. For the sieved soils, the draining branch of $\theta(\psi)$, for pressure heads of 0.2, 0.5, 1, 2, 5, 25, 50, 100, 500 and 1500 kPa, was measured. The water retention curves were fitted, using the SWRC Fit Version 1.2. software (Seki, 2007) (http://seki.webmasters.gr.jp/swrc/), to the unimodal van Genuchten (1980) function (Eq. 2). The α parameters obtained with both techniques for a wetting or draining processes were converted to the opposite water retention curve branch using the hysteresis index developed by Gebrenegus and Ghezzehei (2011).

3. Results and discussion

3.1. Theoretical analysis

The response surfaces (contours) $\phi(\alpha, n)$, $\phi(K_s, n)$, and $\phi(K_s, \alpha)$ for all the boundary condition scenarios are shown in Figure 3, 4 and 5, respectively. The thick red contours represent the ±0.1 mm uncertainty range.

Note that the contours of the S_0 and $S_{-10,0}$ scenarios without the overpressure step showed an elongated experimental uncertainty contour regions. These results prevent defining a unique combination of parameters α-n-K_s with the lowest objective function. In other words, there are infinite combinations of α-n-K_s values within this contour region that can yield almost identical CUI. The results, thus, demonstrate that the low suction experimental conditions are not adequate to uniquely define the hydraulic parameters. However, the response surfaces corresponding to $S_{-50,0}$ and $S_{-100,0}$ scenarios also without the overpressure step exhibit well-defined minimums. Thus, these results suggest that the higher tensions used in these examples provide sufficient information to provide reliable estimates of the soil hydraulic parameters.

The above results indicate that the proposed inverse analysis method provides reliable estimate of hydraulic parameters only within the range of suction that was represented in the experimental data. For example, parameters estimated using the $S_{-10,0}$ provide hyadraulic parameters that are reliable in the range 0 cm to -10 cm of suction. On the other hand, parameters derived using the $S_{-100,,0}$ experiments result in parameters that adequately describe the 0 cm to -100 cm suction range. To check the dependence of the accuracy of the estimated parameters on the range of suction applied in the experiments, we compare the water retention curves of the true cumulative upward infiltration (CUI) with those for the computed CUI using the parameters within the ±0.1 mm uncertainty range (Fig. 6). Note that in all the scenarios, the uncertainty range is very narrow up to approximately the highest suction level applied in the experiments. For this particular soil, the scenario with -100 cm spans most range of the water retention curve, and provides very accurate estimate of the hydraulic

parameters across the board. In this case, the average optimal α and n values estimated for the loam soil, were 0.0358 cm^{-1} and 1.566, respectively, an error of 0.5 and 3%, respectively. From the above discussions, we can conclude that the proposed method provide reliable estimates of hydraulic parameters when the maximum suction is higher than about $-1/\alpha$ cm. To verify this hypothesis, a second simulation on a loamy sand (θ_r = 0.057 m^3 m^{-3}, θ_s = 0.41 m^3 m^{-3}, α = 0.124 cm^{-1}, n = 2.28 and K_s = 0.2432 cm s^{-1}; Simunek et al., 2008) was performed. In this case, pressure heads of -10 cm (15 min), 0 cm (10 min) and 10 cm (5 min) were used. The results confirmed the above described hypothesis, where the -10 cm applied suction, which is higher than the corresponding $-1/\alpha$ value (– 8.06 cm), was enough to provide reliable estimates of hydraulic parameters (Fig. 7). The average optimal α, n values obtained for the loamy sand were 0.0124 cm^{-1} and 2.16, respectively, which means an error of 0.1 and 5%, respectively.

The K_s-α and K_s-n error maps for 0 and 0-10 cm of soil tensions (Fig. 3 and 4 a2 and b2) significantly changed when the overpressure section was included. In these cases, a unique and well defined minimum was found. However, this was not the case of the α-n response surface, which the inclusion of K_s did not limit the experimental uncertainty contour line. To solve this problem, higher negative soil tensions should be considered (Fig. 5 c2 and d2). These analyses demonstrate that for a known K_s, the α and n can be satisfactorily estimated from the inverse analysis of a CUI if moderate soil tensions are applied. In our case, the most accurate estimation of the hydraulic parameters corresponded to a CUI with -100-0 cm of pressure head. To verify this second hypothesis, a third simulation using a known K_s was performed on a clay loam soil (θ_r = 0.095 m^3 m^{-3}, θ_s = 0.41 m^3 m^{-3}, α = 0.019 cm^{-1}, n = 1.31 and K_s = 0.0043 cm min^{-1}; Simunek et al., 2008). The applied soil tensions were -50 cm (270 min), 0 cm (30 min) and 10 cm (40 min). The results confirmed the second hypothesis, where the -50 cm of applied suction, which almost equals to $-1/\alpha$ value (– 52 cm), was enough to provide reliable estimates of the hydraulic parameters (Fig. 8). The optimal α and n values

obtained in this case were 0.0191 cm^{-1} and 1.29, respectively, which supposed an error of 0.52 and 1.5%.

In conclusion, the analysis of the response surfaces for $\phi(K_s, \alpha, n)$ described in the previous paragraphs reveal that two possible ways to estimate K_s, α and n from the inverse analysis of a measured CUI are possible:

(i) Minimization of the objective function $\phi(K_s, \alpha, n)$ on a CUI without overpressure step, when negative enough (e.g. -100 cm) soil pressure heads are supplied.

(ii) Calculation of K_s from the overpressure step at the end of the upward infiltration process according to Eq. (6), and minimization of the objective function $\phi(\alpha, n)$. In this case, medium negative soil pressure heads (e.g. -30 cm) could be used. The theoretical analysis performed on the loam soil demonstrated that the average error to calculate K_s from the overpressure ramp of the CUI according to the Darcy's law was 0.23%.

3.2. Laboratory experiment

Values of the soil bulk density (ρ_b) and the saturated and residual water contents of the different soils used in the laboratory experiment in the tension sorptivimeter and TDR-cell are summarized in Table 3. Due to the maximum tension allowed by the tension sorptivimeter ranged between 30 and 40 cm, the soil hydraulic parameters were estimated according to the procedure ii). This involved calculating K_s from the overpressure step at the end of the upward infiltration process. The K_s values calculated using the Darcy's law are shown in Table 3. The maximum and minimum K_s values corresponded to the coarse sand and the silt-gypseous soils, respectively. As example, Figure 9a and b shows the α-n responses surfaces for the objective function $\phi(\alpha, n)$ and the comparison between the experimental and optimal cumulative upward infiltration obtained for the coarse sand and the 1-mm sieved loam and silt-gypseous soil. Overall, good fittings between the experimental and optimal

cumulative upward infiltrations (Fig. 9a) were obtained. Except for the sand, a well defined minimum (Fig. 9b) was observed in the error maps. The elongated contour line observed in the coarse sand indicates that *n* values ranged between 3.0 to 3.5 give very similar infiltration curves. This behavior can be explained because of quasi identical water retention curve shapes are obtained for the *n* values ranging between 3.0 and 3.5. The α and *n* values estimated for the five soils with the global optimization analysis, after being recalculated for a draining process (Table 3), were within the same order of magnitude to those values obtained with the pressure cell method. A significant relationship between the α ($p < 0.02$) and *n* ($p < 0.001$) values estimated with the pressure cell and the tension soptivimeter was found (Fig. 10). The higher significance observed in *n* could be due to the fact that the *n* parameter is more related to the soil texture (Jirku et al., 2013) and α is more associated to the soil structure. Thus, the lower α values obtained with the pressure cell method (Fig. 10) may associated to the soil macroporosity collapse during the measurements. The shorter measurement times with the sorptivimeter could have minimized the soil micro-structure changes during the soil wetting process, and better preserve its internal architecture. Overall, the error between the α (in logarithm scale) and *n* parameters estimated with the inverse analysis and those measured with the pressure chamber were 3.1 and 6.1%, respectively. As example, Figure 10 shows the relationship between the S_e curves estimated with both techniques in the 1-mm sieved loam soil.

4. Conclusions

This paper presents a modified method to estimate the soil hydraulic parameters (K_s, α, *n*) from the inverse analysis of a multiple tension cumulative upward infiltration (CUI), without using tensiometers. Using the HYDRUS-2D software, the method was tested on a theoretical loam soil for different tensions with and without an overpressure step at the end of the simulations. Next, the method was validated in laboratory on five porous media with different texture. This work

demonstrated that the soil hydraulic parameters can be satisfactorily estimated from a CUI without an overpressure step at the end of the infiltration process if negative enough pressure heads (e.g. -100 cm) to correctly define the water retention curve are applied. Alternatively, if only medium negative soil pressure heads (e.g. -40 cm) are allowed, K_s can be calculated from the overpressure step of a CUI, and α and n can be estimated by minimization of the $\phi(\alpha, n)$ objective function. The laboratory experiments allowed a satisfactory validation of the technique. Compared to existent laboratory methods, the tension sorptivimeter resulted to be a relatively fast and simple method. The time needed to measure a CUI run about 1-2 hours, and the analysis of the measured curves, which is relatively fast if a computer cluster is available, could be improved if a more efficient optimization method was used. Compared to the Young et al. (2002) procedure, which requires similar experimental times, the method here presented allows working with smaller soils cores and does not need to employ tensiometers. This makes this technique to be less expensive and simpler handling. However, additional efforts should be done to determine, for instance, the influence of the absorption time on the hydraulic properties estimations, or to study new combinations of tensions to improve the CUI optimizations. On the other hand, the highly tension used at the beginning of the experiment, which is close to the bubbling pressure (tension) of the nylon mesh, makes that only soil samples that ensure good contact between the nylon surface and the soil (e.g. sieved soils) can be used. This problem could be solved by starting the experiment at saturation conditions. To this end, alternative tension sorptivimeter designs should be developed. Finally, because of this method needs to previously select the tensions to be used, the application of this method to all types of soil is, in any case, complex. That is, the tensions needed to characterize, for instance, a sand are different to those for a loam soil. For these reason, additional efforts are needed to develop alternative laboratory designs that allow automating the tensions to be applied, independently to the soil characteristics.

Acknowledgements

We would like to thank to the Área de Informática Científica de la SGAI (CSIC) for their technical support in the numerical analysis, and also to Ricardo Gracia, María Josefa Salvador and María Victoria López for their technical help to develop this paper.

References

Casey F.X.M., and N.E. Derby. 2002. Improved design for an automated tension infiltrometer. *Soil Science Society of American Journal* **66**: 64–67.

Carsel, R.F., and R.S. Parrish. 1988. Developing joint probability distributions of soil water retention characteristics. *Water Resources Research* **24**: 755-769.

Gebrenegus, T.,. Ghezzehei, T.A. 2011. An index for degree of hysteresis in water retention. *Society of American Journal* **75**:2122–2127

Horst, R., Romeijn, H. E. (Eds.). 2002. Handbook of global optimization (Vol. 2). Springer Science & Business Media.

Hunt, A.G., Ewing, R.P., Horton, R. 2013. What's wrong in soil physics?. *Science Society of America Journal* **77:** 1877-1887.

Hudson, D.B., Wierenga, P.J., Hills, R.G. 1996. Unsaturated hydraulic properties from upward flow into soil cores. *Society of American Journal* **60**: 388-396.

Jirku, V., Kodesová, R., Nikodem, A., Mühlhanselová, M., Zigová, A., 2013. Temporal variability of structure and hydraulic properties of topsoil of three soil types. *Geoderma* **204**, 43-58.

Klute A., 1986. Water retention curve: laboratory methods. In, Methods of Soil Analysis. Part 1. (Ed. A. Klute), SSSA Book Series No. 9. Soil Science Society of America, Madison WI.

Klute A., Dirksen, C. 1986. Hydraulic conductivity and diffusivity: laboratory methods. In, Methods of Soil Analysis. Part 1. (Ed. A. Klute), SSSA Book Series No. 9. Soil Science Society of America, Madison WI.

Lichtner, P.C., Steefel, C.I. Oelkers E.H. 1996. Reactive Transport in Porous Media. Mineralogical Society of America , p. 5.

Moret-Fernández, D., Vicente, J., Latorre B., Herrero, J., Castañeda, C., Lópe, M.V. 2012. TDR pressure cell for monitoring water content retention curves on undisturbed soil samples. *Hydrological Process*. **26**: 246-254.

Ramos, T.B., Gonçalves, M. C., Martins, J. C., van Genuchten, M. Th., Pires, F. P. 2006. Estimation of soil hydraulic properties from numerical inversion of tension disk infiltrometer data. *Science Society of American Journal* **5**: 684-696.

Rashid, N.S.A., Askari, M., Tanaka, T., Simunek, J., van Genuchten, M.T. 2015. Inverse estimation of soil hydraulic properties under oil palm trees. *Geoderma* **241-242**: 306-312.

Seki, K., 2007. SWRC fit – a nonlinear fitting program with a water retention curve for soils having unimodal and bimodal pore structure. *Hydrological and Earth System Science* **4**: 407-437.

Simunek, J., van Genuchten, M.T. 1996. Estimating unsaturated soil hydraulic properties from tension disc infiltrometer data by numerical inversion. *Water Resources Research* **32**: 2683-2696.

Simunek, J., vam Genuchten, M.T. 1997. Estimating unsaturated soil hydraulic properties from multiple tension disc infiltrometer data. *Soil Science* ***1*****62**: 383-398.

Simunek, J., Wendroth, O., Wlypler, N., van Genuchten, M.T.. 2001. Non-equilibrium water flow characterized by means of upward infiltration experiments. *European Journal of Soil Science* **52**: 13-24.

Simunek, J., van Genuchten, M.T., Sejna, M., 2008. Development and applications of the HYDRUS and STANMOD software packages and related codes. *Vadose Zone Journal* **7**: 587–600.

van Genuchten, M.T., 1980. A closed-form equation for predicting the hydraulic properties of unsaturated soils. *Soil Science Society of America Journal* **44**: 892-898.

Wand, X., Benson, C.H., 2004. Leak-free pressure plate extractor for measuring the soil water characteristic curve. *Geotechnical Testing Journal* **27**: 1-9.

Young, M.H., Karagunduz, A., Siumunek, J., Pennell, K.D. 2002. A modified upward infiltration method for characterizing soil hydraulic properties. *Soil Science Society of America Journal* **66**: 57–64.

Figures captions

Figure 1. Examples of cumulative upward infiltration (CUI) generated by HYDRUS-2D in a theoretical loam soil for the different scenarios of Table 1 without (No oversat) and with oversaturation (Oversat) step at the end of the experiment.

Figure 2. Diagram of the tension sorptivimeter

Figure 3. Contours of objective function $\phi(K_s, \alpha, n)$ for the cumulative upward infiltration of a theoretical loam soil in the α-n plane at pressure heads of a) 0, b) -10 and 0 , c) -50 and 0, d) -100 and 0 cm, without (1) and plus (2) an overpressure head of 5 cm from the soil surface. Contour lines denote error values of 0.25, 0.5, 1, 2, 3, and 5 mm, respectively. Thick red line corresponds to the experimental uncertainty contour line (0.1 mm) due to water level measurement.

Figure 4. Contours of objective function $\phi(K_s, \alpha, n)$ for the cumulative upward infiltration of a theoretical loam soil in the K_s-n plane at pressure heads of a) 0, b) -10 and 0 , c) -50 and 0, d) -100 and 0 cm, without (1) and plus (2) an overpressure head of 5 cm from the soil surface. Contour lines denote error values of 0.25, 0.5, 1, 2, 3, and 5 mm, respectively. Thick red line corresponds to the experimental uncertainty contour line (0.1 mm) due to water level measurement.

Figure 5. Contours of objective function $\phi(K_s, \alpha, n)$ for the cumulative upward infiltration of a theoretical loam soil in the K_s-α plane at pressure heads of a) 0, b) -10 and 0 , c) -50 and 0, d) -

100 and 0 cm, without (1) and plus (2) an overpressure head of 5 cm from the soil surface. Contour lines denote error values of 0.25, 0.5, 1, 2, 3, and 5 mm, respectively. Thick red line corresponds to the experimental uncertainty contour line (0.1 mm) due to water level measurement.

Figure 6. Water retention curves corresponding to the cumulative upward infiltration of a theoretical loam soil calculated from the α-n values included within 0.1 mm contour line of the α-n error map (Fig. 5) for: a) 0, b) -10 and 0, c) -50 and 0 cm, and d) -100 and 0 cm of pressure heads. Red curve correspond to the theoretical water retention curve. Vertical line denotes the maximum suction applied to the soil water absorption process.

Figure 7. Contours of objective function $\phi(K_s, \alpha, n)$ for the cumulative upward infiltration of a theoretical loamy sand soil in the a) K_s-n, b) α-n and c) K_s-α planes at pressure heads of -10 and 0 cm. Contour lines denote error values of 0.25, 0.5, 1, 2, 3, and 5 mm, respectively. Thick red line corresponds to the experimental uncertainty contour line (0.1 mm) due to water level

Figure 8. Contours of objective function $\phi(\alpha, n)$ for the cumulative upward infiltration of a theoretical clay loam soil in the α-n plane at pressure heads of -50, 0 and 10 cm. Contour lines denote error values of 0.25, 0.5, 1, 2, 3, and 5 mm, respectively. Thick red line corresponds to the experimental uncertainty contour line (0.1 mm) due to water level measurement.

Figure 9. a) Experimental soil cumulative upward infiltration (CUI) (circles) and the optimal modelled curves (line). Numbers within these figures denote the soil tensions applied at the bottom of the soil core. b) Contour of the objective function $\alpha(\alpha, n)$ for the CUI in the α-n

plane estimated on the experimental coarse sand, and 1-mm sieved loam and silt gypseous soils subjected to different soil tensions at the bottom of the soil core. The K_s has been calculated form the CUI overpressure step. Thick red line corresponds to the experimental uncertainty contour line of 0.5 mm for the coarse sand and and loam soil and 1.0 mm for the silt-gypseous soil.

Figure 10. Relationship between the a) α and b) n values estimated with the pressure cell and the corresponding values estimated with tension soptivimeter for the coarse and fine sand, and 1-mm sieved loam, clay loam and silt-gypseous soils.

Figure 11. Comparison between the effective saturation (S_e) curves measured on a 1-mm sieved loam soil with the pressure cell (circles) and the corresponding curve obtained by inverse analysis (line) of a multiple tension cumulative upward infiltration (Fig. 8b) measured with the tension sorptivimeter.

Table 1. Pressure heads at the bottom boundary condition and times intervals used in theoretical simulations on a loam soil.

Scenario	Pressure heads cm	Time per tension min
S_0	0	30
$S_{0\text{-}10}$	-10, 0	80, 30
$S_{0\text{-}50}$	-50, 0	270, 30
$S_{0\text{-}100}$	-100, 0	470, 30

Table 2. Soil properties of the studied soil, applied soil tensions and the corresponding infiltration times.

Texture [a]	Sand	Silt	Clay	$CaCO_3$	Gypsum	Organic carbon	Soil tensions	Interval times
	g kg^{-1}						cm	min
Coarse-sand	953	33	14	-	-	-	-15, 0, 7	30, 16, 4
Fine-and	962	27	11	-	-	-	-12, 0, 7	30, 4, 6
Loam	280	470	250	527	-	11.7	-40, 0, 9	185, 16, 35
Clay loam	205	497	298	228	-	19.9	-35, 0, 9	152, 12, 10
Silt-gypseous	316	591	129	10	703	1.5	-35, 0, 7	30, 50, 24

[a] USDA classification;

Table 3. Soil bulk density (ρ_b), saturated and residual water contents (θ_s and θ_r), saturated hydraulic conductivity (K_s) and the van Genuchten (1980) water retention curve parameters (α, n) estimated with the tension soptivimeter (TS) for a wetting process, and the corresponding values measured with a TDR-pressure cell (PC) in a wetting (sands) and draining (sieved soils) process. Blond italics letters indicate the corresponding α values calculated from the measured α parameter using the Gebrenegus and Ghezzehei (2011) model.

Soil	Method	Process	ρ_b	θ_s	θ_r	K_s	n	α_w [a]	α_d [b]
			(g cm^{-3})	(cm^3 cm^{-3})		(cm min^{-1})	(cm^{-1})		
Coarse-sand	PC	Draining	1.51	0.40	0.02 [c]	-	2.94	0.066	***0.033***
	TS	Wetting	1.50	0.43	0.02	1.709	3.20	0.084	***0.041***
Fine-sand	PC	Draining	1.57	0.38	0.02	-	2.33	0.078	***0.039***
	TS	Wetting	1.54	0.43	0.02	0.763	2.71	0.113	***0.056***
Loam	PC	Draining	1.19	0.48	0.16	-	1.64	***0.076***	0.039
	TS	Wetting	1.06	0.53	0.01	0.108	1.52	0.100	***0.050***
Clay loam	PC	Draining	1.31	0.52	0.36	-	1.32	***0.102***	0.055
	TS	Wetting	1.32	0.49	0.02	0.630	1.43	0.124	***0.065***
Silt- gypseous	PC	Draining	1.07	0.49	0.41	-	1.27	***0.047***	0.026
	TS	Wetting	0.95	0.46	0.02	0.110	1.23	0.042	***0.024***

[a] α value for a wetting process
[b] α value for a draining process
[c] Estimated with the SWRC-fit software (Seki, 2007)

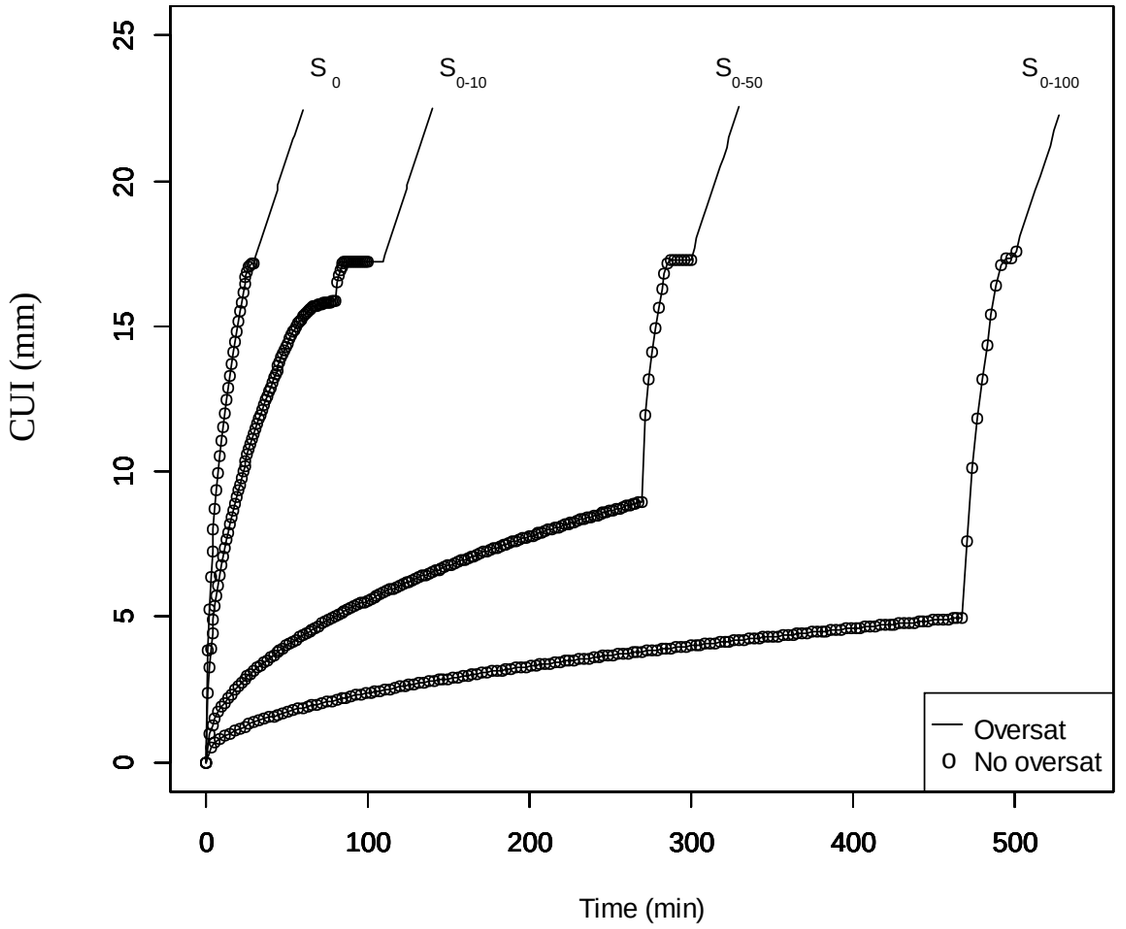

Figure 1. Examples of cumulative upward infiltration (CUI) generated by HYDRUS-2D in a theoretical loam soil for the different scenarios of Table 1 without (No oversat) and with oversaturation (Oversat) step at the end of the experiment.

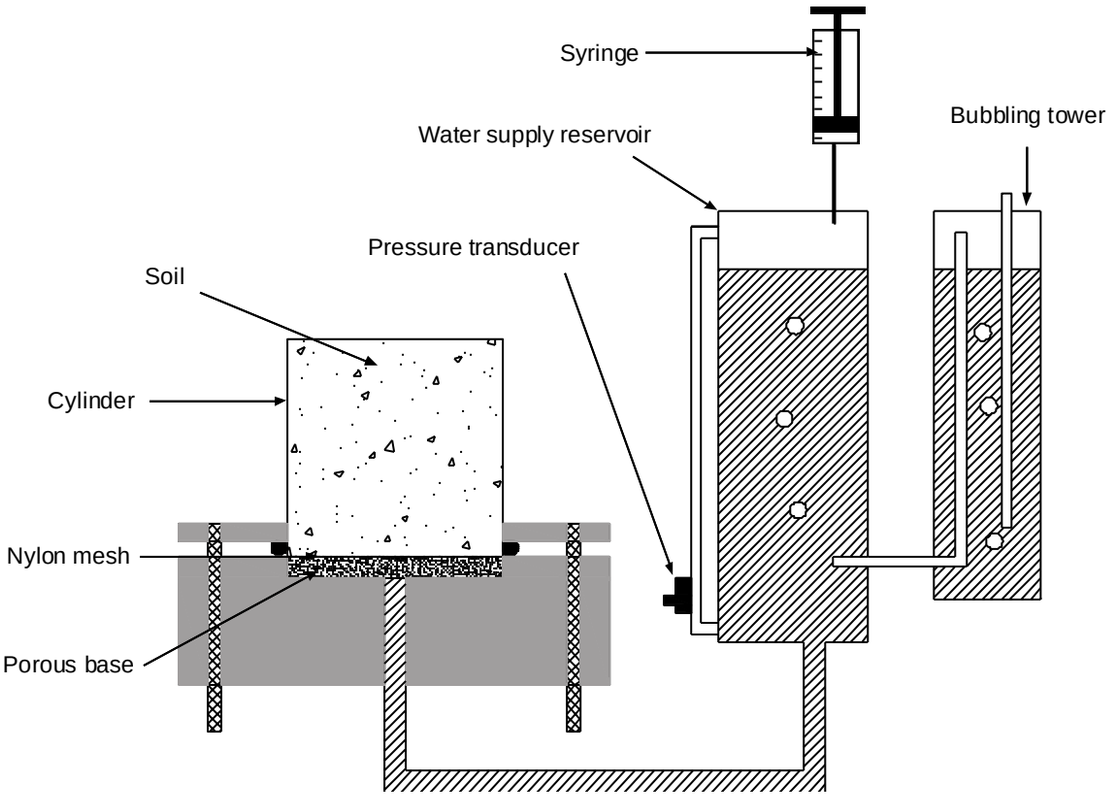

Figure 2. Diagram of the tension sorptivimeter

1

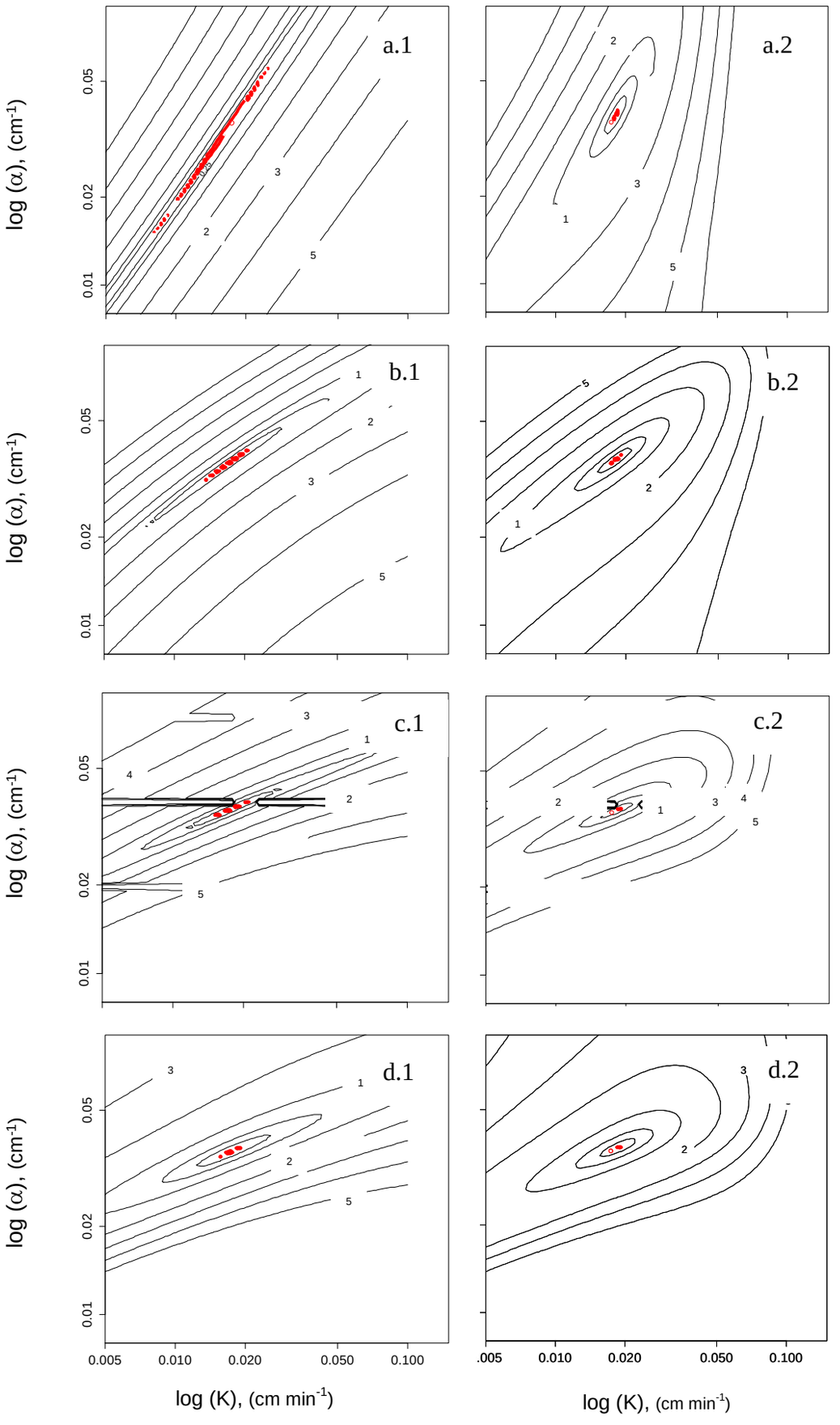
a.1
a.2
b.1
b.2
c.1
c.2
d.1
d.2
log (α), (cm-1)
log (K), (cm min-1)
0.01
0.02
0.05
0.005
0.010
0.020
0.050
0.100

Figure 3. Contours of objective function $\phi(K_s, \alpha, n)$ for the cumulative upward infiltration of a theoretical loam soil in the α-n plane at pressure heads of a) 0, b) -10 and 0 , c) -50 and 0, d) -100 and 0 cm, without (1) and plus (2) an overpressure head of 5 cm from the soil surface. Contour lines denote error values of 0.25, 0.5, 1, 2, 3, and 5 mm, respectively. Thick red line corresponds to the experimental uncertainty contour line (0.1 mm) due to water level measurement.

1

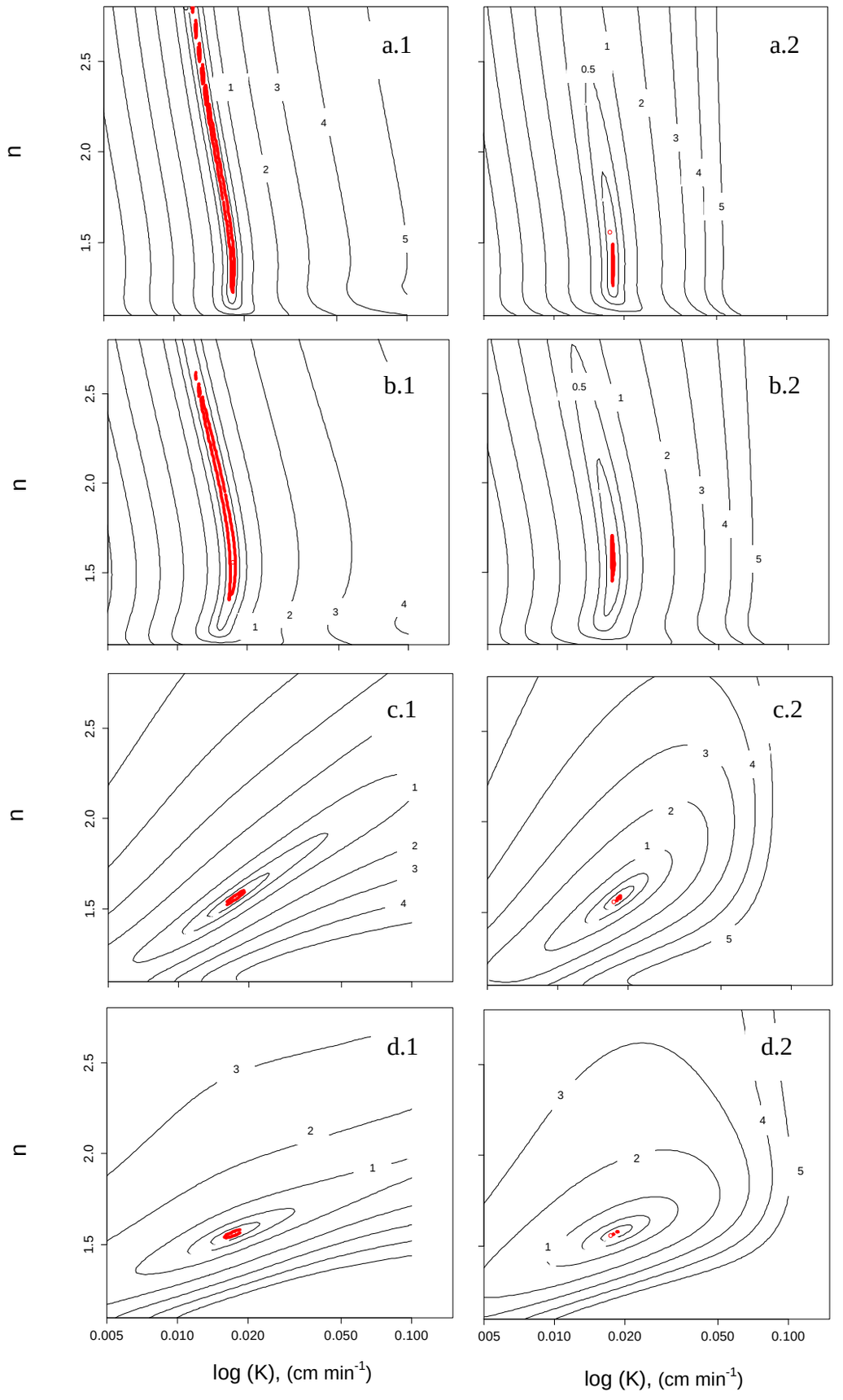
a.1
a.2
b.1
b.2
c.1
c.2
d.1
d.2
n
2.5
2.0
1.5
0.005
0.010
0.020
0.050
0.100
log (K), (cm min-1)

Figure 4. Contours of objective function $\phi(K_s, \alpha, n)$ for the cumulative upward infiltration of a theoretical loam soil in the K_s-n plane at pressure heads of a) 0, b) -10 and 0 , c) -50 and 0, d) -100 and 0 cm, without (1) and plus (2) an overpressure head of 5 cm from the soil surface. Contour lines denote error values of 0.25, 0.5, 1, 2, 3, and 5 mm, respectively. Thick red line corresponds to the experimental uncertainty contour line (0.1 mm) due to water level measurement.

1

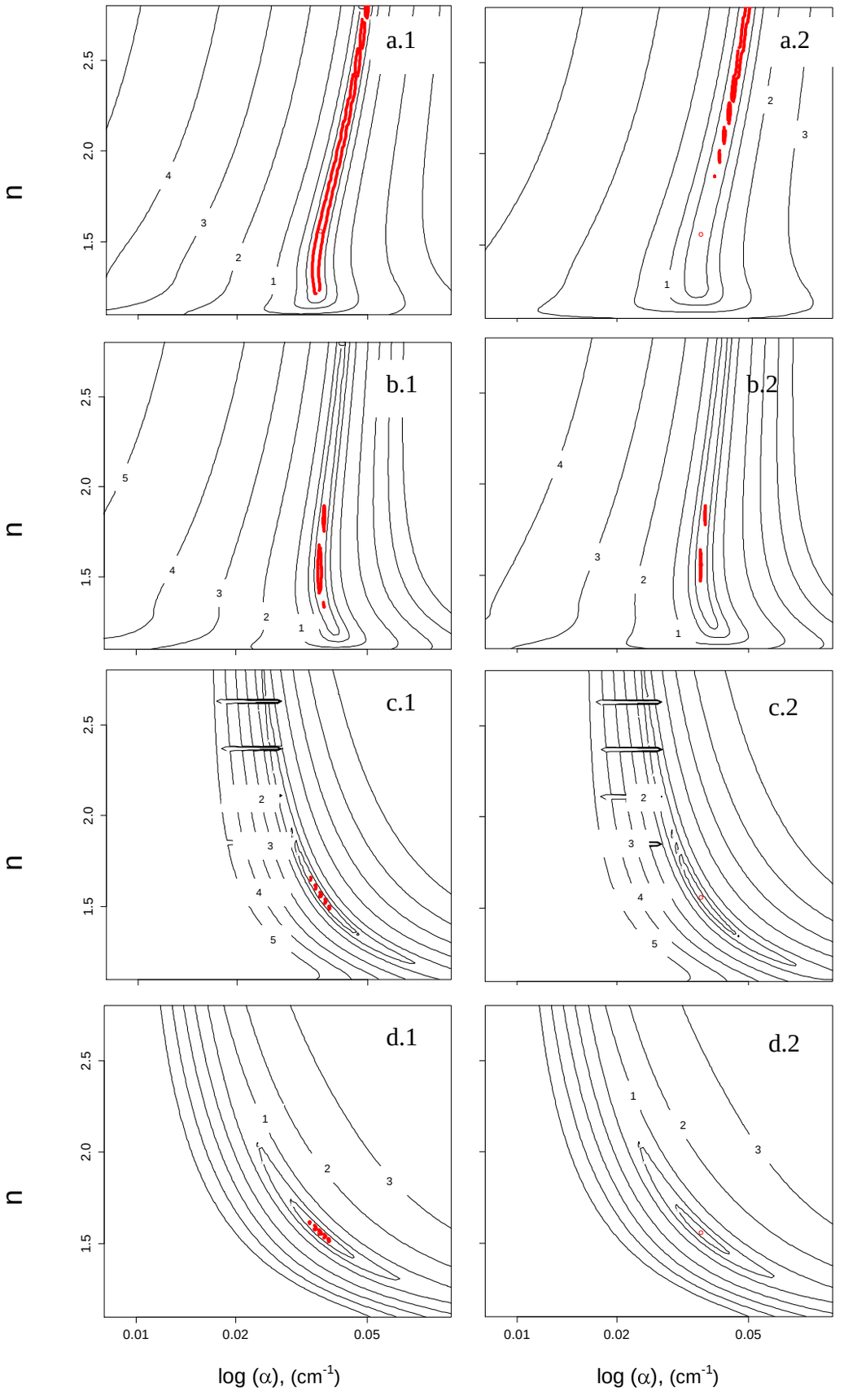

Figure 5. Contours of objective function $\phi(K_s, \alpha, n)$ for the cumulative upward infiltration of a theoretical loam soil in the K_s-α plane at pressure heads of a) 0, b) -10 and 0 , c) -50 and 0, d) -100 and 0 cm, without (1) and plus (2) an overpressure head of 5 cm from the soil surface. Contour lines denote error values of 0.25, 0.5, 1, 2, 3, and 5 mm, respectively. Thick red line corresponds to the experimental uncertainty contour line (0.1 mm) due to water level measurement.

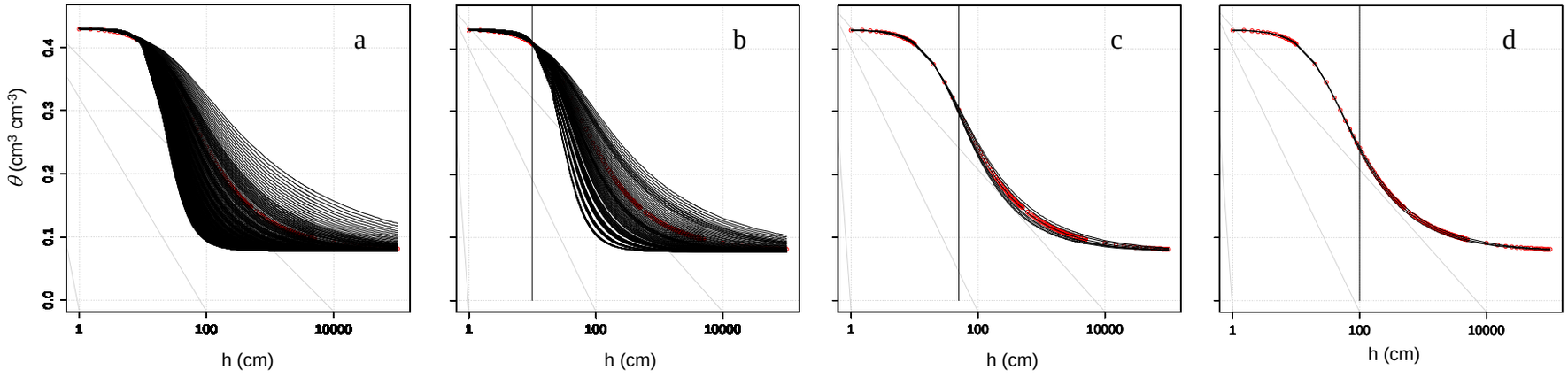

Figure 6. Water retention curves corresponding to the cumulative upward infiltration of a theoretical loam soil calculated from the α-n values included within 0.1 mm contour line of the α-n error map (Fig. 5) for: a) 0, b) -10 and 0, c) -50 and 0 cm, and d) -100 and 0 cm of pressure heads. Red curve correspond to the theoretical water retention curve. Vertical line denotes the maximum suction applied to the soil water absorption process.

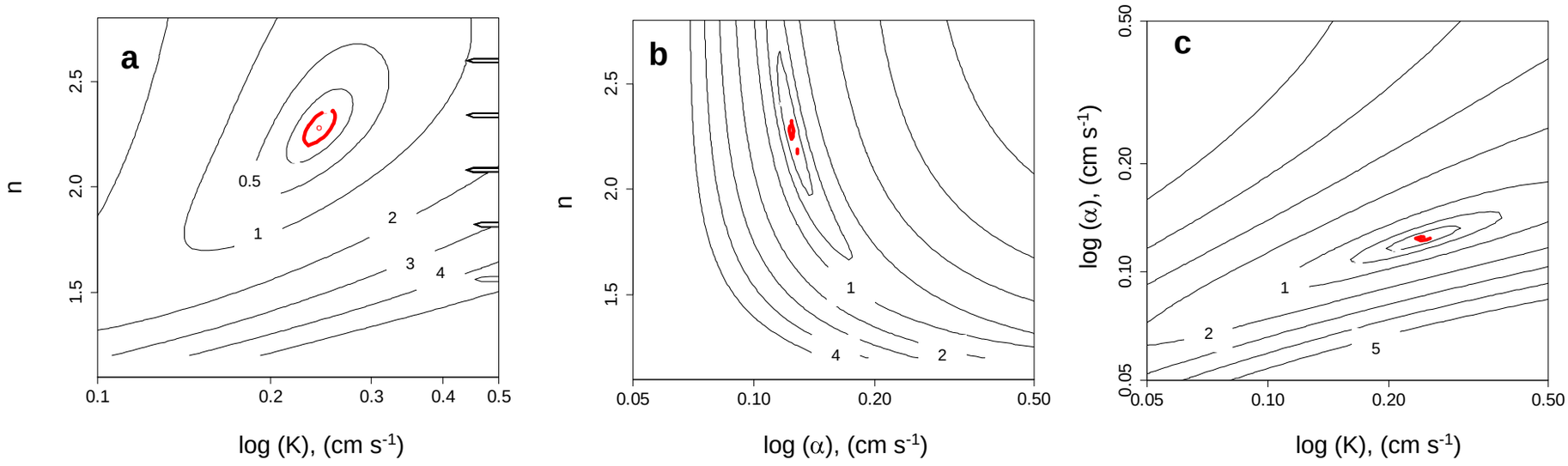

Figure 7. Contours of objective function $\phi(K_s, \alpha, n)$ for the cumulative upward infiltration of a theoretical loamy sand soil in the a) K_s-n, b) α-n and c) K_s-α planes at pressure heads of -10 and 0 cm. Contour lines denote error values of 0.25, 0.5, 1, 2, 3, and 5 mm, respectively. Thick red line corresponds to the experimental uncertainty contour line (0.1 mm) due to water level

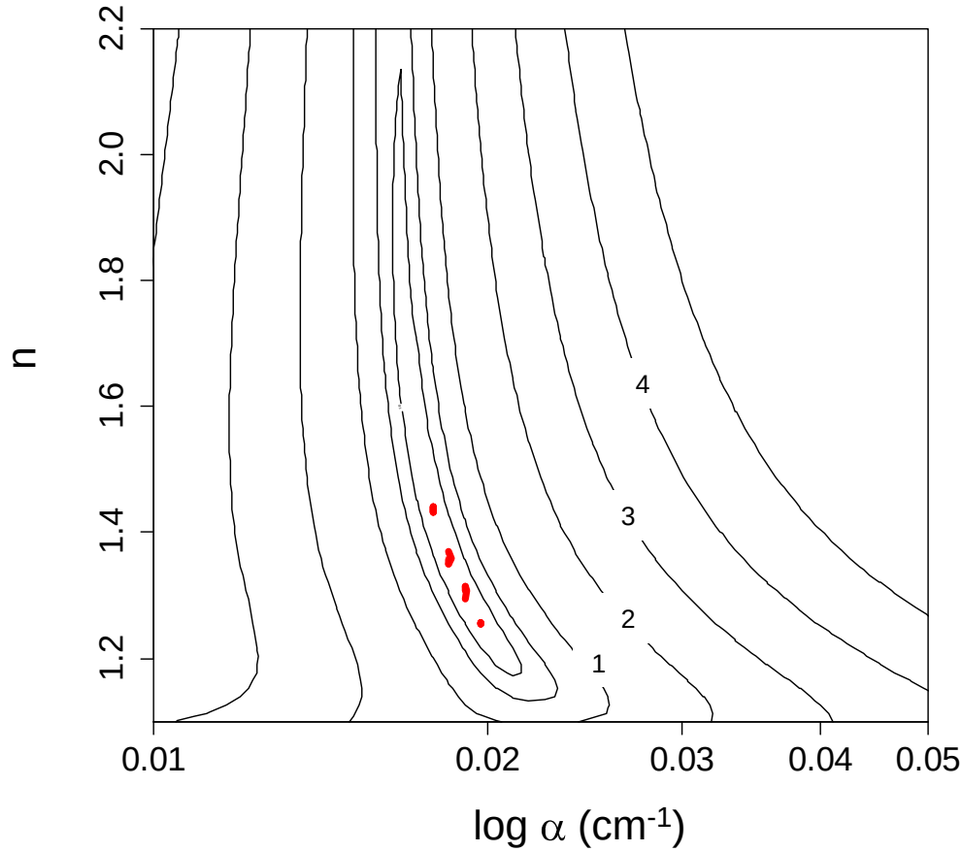

Figure 8. Contours of objective function $\phi(\alpha, n)$ for the cumulative upward infiltration of a theoretical clay loam soil in the α-n plane at pressure heads of -50, 0 and 10 cm. Contour lines denote error values of 0.25, 0.5, 1, 2, 3, and 5 mm, respectively. Thick red line corresponds to the experimental uncertainty contour line (0.1 mm) due to water level measurement.

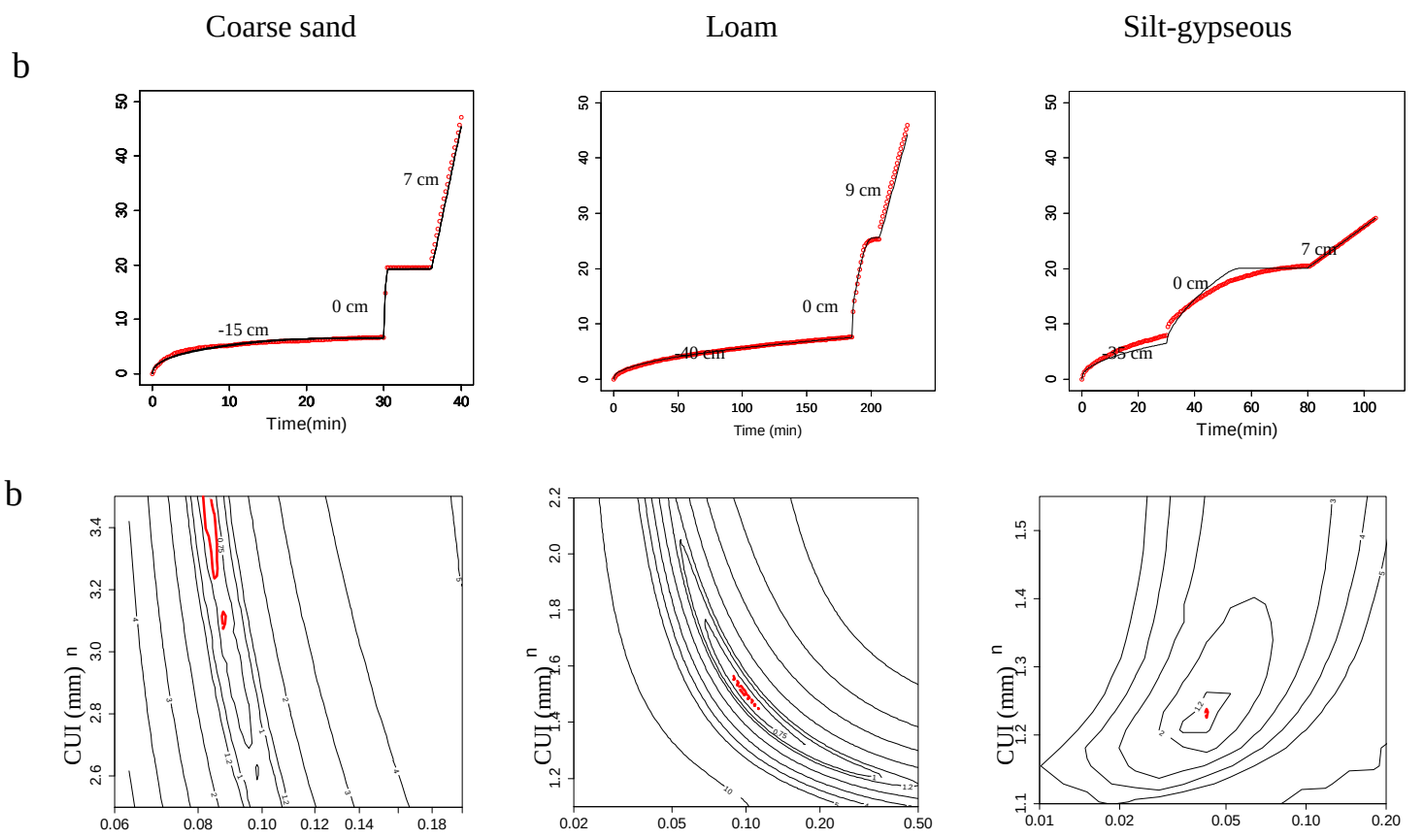

Figure 9. a) Experimental soil cumulative upward infiltration (CUI) (circles) and the optimal modelled curves (line). Numbers within these figures denote the soil tensions applied at the bottom of the soil core. b) Contour of the objective function $\phi(\alpha, n)$ for the CUI in the α-n plane estimated on the experimental coarse sand, and 1-mm sieved loam and silt gypseous soils subjected to different soil tensions at the bottom of the soil core. The K_s has been calculated form the CUI overpressure step. Thick red line corresponds to the experimental uncertainty contour line of 0.5 mm for the coarse sand and and loam soil and 1.0 mm for the silt-gypseous soil

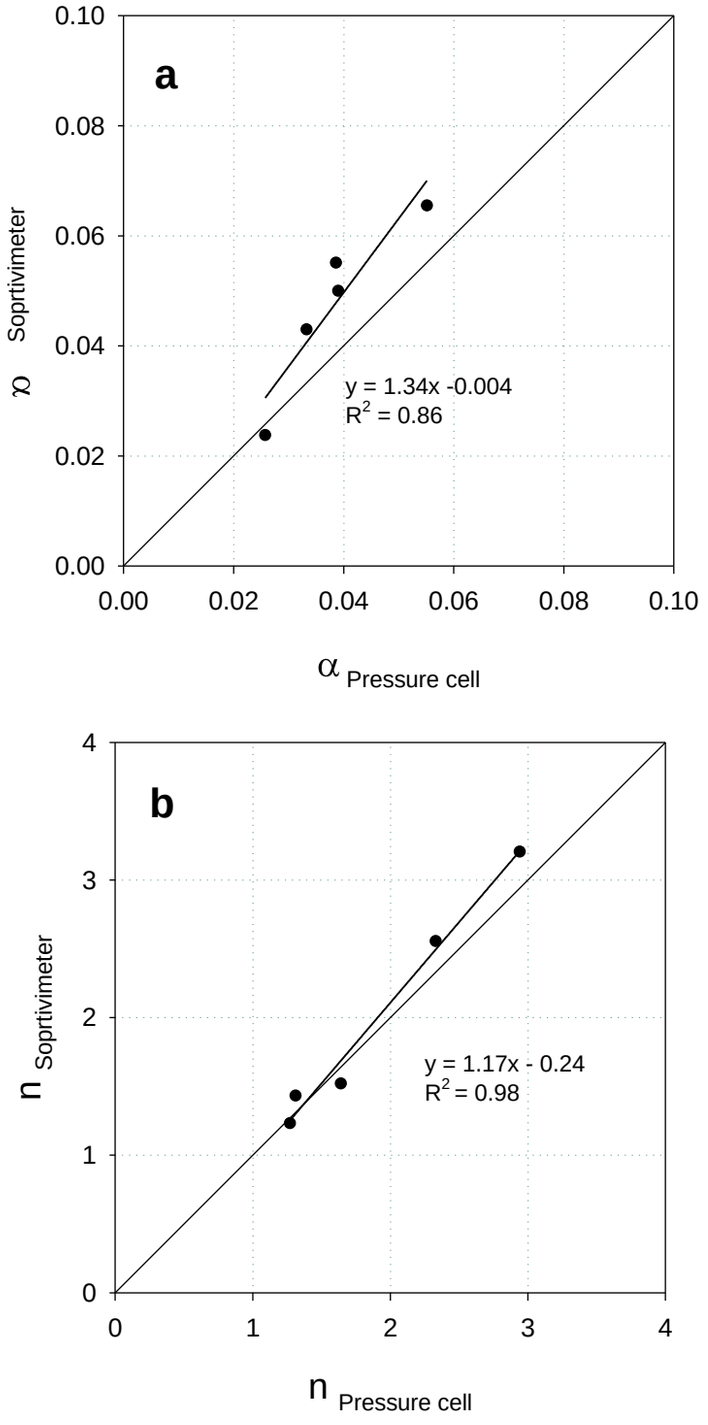

Figure 10. Relationship between the a) α and b) n values estimated with the pressure cell and the corresponding values estimated with tension soptivimeter for the coarse and fine sand, and 1-mm sieved loam, clay loam and silt-gypseous soils.

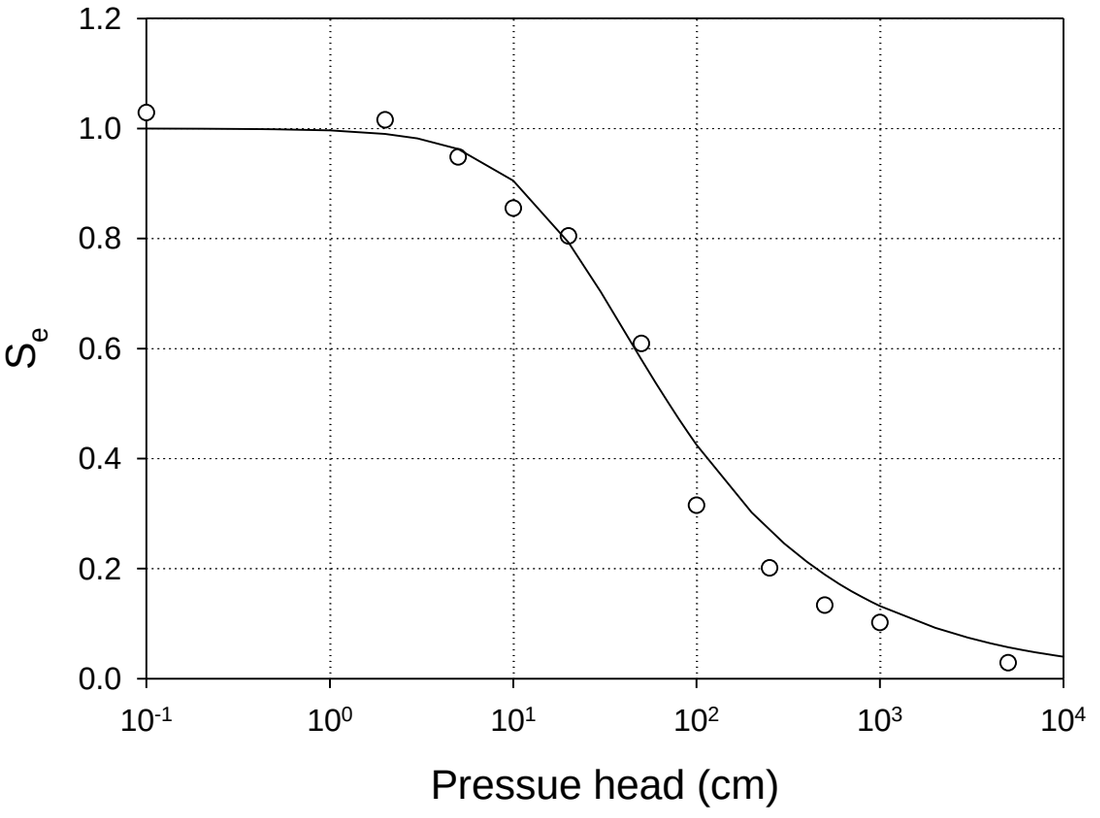

Figure 11. Comparison between the effective saturation (S_e) curves measured on a 1-mm sieved loam soil with the pressure cell (circles) and the corresponding curve obtained by inverse analysis (line) of a multiple tension cumulative upward infiltration (Fig. 8b) measured with the tension sorptivimeter.